04,09

Structural and spectral characteristics of $La_{0.99-x}Y_xEu_{0.01}BO_3$ orthoborates

© S.Z. Shmurak, V.V. Kedrov, A.P. Kiselev, T.N. Fursova, I.I. Zver'kova

Osipyan Institute of Solid State Physics RAS,
Chernogolovka, Russia

E-mail: shmurak@issp.ac.ru

Received April 22, 2022
Revised April 22, 2022
Accepted April 24, 2022

The structure, IR absorption, luminescence, and luminescence excitation spectra of $La_{0.99-x}Y_xEu_{0.01}BO_3$ orthoborates synthesized at 970°C were studied at $0 \le x \le 0.99$. An increase in x leads to a sequential change of the structural state of these compounds. At $0 \le x \le 0.1$, the samples are single-phase and have the aragonite structure. Within the range of $0.1 < x \le 0.8$, the samples are two-phase: the vaterite phase is observed along with the aragonite structure. At $0.8 < x \le 0.99$, the samples are single-phase and have the vaterite structure. Correspondence between the structure and spectral characteristics of these compounds was established. It is demonstrated that with an increase in the Y^{3+} concentration, the vaterite phase is formed first in the bulk of microcrystals having the aragonite structure and then in the entire sample. It is shown for the first time that a band with the maximum of 469 nm is observed in the luminescence excitation spectrum (LES) of samples having the vaterite structure and is absent in samples having the aragonite structure. It is revealed that a band in the luminescence spectrum, corresponding to the $^5D_0 \rightarrow {}^7F_0$ electron transition, as well as 469 nm-band in the LES, can be an indicator of the structural state of the sample.

Keywords: rare earth orthoborates, X-ray diffraction analysis, crystal structure, IR spectroscopy, luminescence spectra.

DOI: 10.21883/PSS.2022.08.54611.359

1. Introduction

Directional changing of spectral characteristics of polymorphous phosphors, used as active elements in light-emitting-diode light sources, is extremely important for optimization of light-emitting diodes' spectral characteristics. One of the most efficient methods for directional changing of the radiation spectrum of polymorphous phosphors with optically active centers is changing of their structural state, since each structural modification corresponds to a specific luminescence spectrum. For instance, the luminescence spectrum of the vaterite modification of rare earth element orthoborates $ReBO_3(Eu)$, where Re = Gd, Tb, Dy, Eu, Y, Lu, has three bands in the wavelength range of 588–596; 608–616; 624–632 nm, each of which consists of several narrow lines [1–5]. At the same time, the luminescence spectrum of the calcite modification $(Lu, In)BO_3(Eu)$ contains two narrow lines with $\lambda_{max} \sim 590$ and 596 nm [6–8]. According to the different spectral composition of luminescence of the above-mentioned borates, the vaterite modification is characterized by red luminescence, while the calcite structure — by orange luminescence. The luminescence spectrum of lanthanum orthoborate ($LaBO_3(Eu)$), which has the aragonite structure (space group $Pnam$), the most intensive are the bands with $\lambda_{max} = 589.4$, 591 and 592.6 nm, which corresponds to the $^5D_0 \rightarrow {}^7F_1$ electron transition, as well as number of bands in the wavelength range of 608–628 nm ($^5D_0 \rightarrow {}^7F_2$) [9–12]. It should be noted that the spectral composition of luminescence of $LaBO_3(Eu)$, which has the aragonite structure, is closer to the spectral composition of luminescence of $ReBO_3(Eu)$ compounds having the vaterite structure than to orthoborates having the calcite structure.

The luminescence excitation spectra (LES) of the main luminescence bands of various structural modifications of $ReBO_3(Eu)$ borates in the ultraviolet spectrum region has wide bands (charge transfer bands (CTB)), the maxima of which for the aragonite, vaterite and calcite phases are at the wavelengths of 283, 242 and 254 nm respectively. LES of these compounds also contain several narrow bands in the wavelength range of 290–500 nm, corresponding to resonance excitation of Eu^{3+} ions. The most intensive bands in the long-wave spectrum region are $\lambda_{ex} = 394$ nm ($^7F_0 \rightarrow {}^5L_6$); 466.5 nm ($^7F_0 \rightarrow {}^5D_2$) [1–5,10,11]. It should be also noted that the normalized intensities of the LES bands in orthoborates having the aragonite and vaterite structure are close, while for the calcite structure the intensity of the charge transfer band is significantly higher than the resonance bands. The presence of the dominant short-wave band is an important feature of the LES samples having the calcite structure. Me^{3+} ions in the calcite structure $MeBO_3$ (Me = Lu, In) are surrounded by six oxygen ions. Re^{3+} ions in $ReBO_3$ compounds, where Re = Gd, Tb, Dy, Eu, Y, Lu, having the vaterite structure, are surrounded by eight oxygen ions [13–15], while Re^{3+} ions in orthoborates having the aragonite structure $ReBO_3$, where Re = La, Pr, Nd, are surrounded by nine oxygen ions [16–19]. Boron ions in calcite and aragonite structures

have trigonal coordination by oxygen — $(BO_3)^{3-}$ [20]. At the same time, three boron atoms with a tetrahedral environment by oxygen in the vaterite structure make up a $(B_3O_9)^{9-}$ group in the form of a three-dimensional ring [21].

The $LaBO_3$ orthoborate has two phase states: the low-temperature orthorhombic aragonite phase (space group $Pnam$) and the high-temperature monoclinic phase (space group $P2_1/m$), to which $LaBO_3$ transforms at 1488°C [13–16]. The low-temperature $PrBO_3$ and $NdBO_3$ phases, like lanthanum orthoborate, have the aragonite structure [22–24]. Lutetium borate ($LuBO_3$) has two stable structural modifications: vaterite formed during synthesis of $LuBO_3$ at $T = 750-850$°C, and calcite formed at $T = 970-1100$°C [14–16].

Papers [8,4,5,25,26] studied solid solutions of lutetium borate and borates having only one modification of lutetium borate: either calcite ($InBO_3$) or vaterite ($ReBO_3$, Re = Eu, Gd, Tb, Dy, Y). An increase of the concentration of In^{3+} ions in $Lu_{0.98-x}In_xEu_{0.02}BO_3$ compounds, synthesized at 780°C (the temperature of presence of vaterite $LuBO_3$), leads to an increase of the calcite phase. At $0 \le x < 0.04$, the solid solution is single-phase and has the vaterite structure (space group $C2/c$), at $0.04 \le x \le 0.1$ it becomes two-phase and contains the vaterite and calcite phases, while at $x > 0.1$ the $Lu_{0.98-x}In_xEu_{0.02}BO_3$ orthoborate has the calcite structure (space group $R\bar{3}c$).

At the same time, solid solutions of $Lu_{1-x}Re_xBO_3$ (Re = Eu, Gd, Tb, Dy and Y) at $x > 0.15-0.2$, synthesized at $T = 970-1100$°C (the temperature of presence of the $LuBO_3$ calcite phase), are crystallized in the vaterite structure. Two types of crystalline phases successively change with a rise of the Re concentration: at $0 \le x \le 0.05-0.1$ the solid solution of orthoborates is single-phase and has the calcite structure (space group $R\bar{3}c$); at $0.05-0.1 < x \le 0.1-0.25$, the vaterite phase (space group $C2/c$) appears along with the calcite structure, while at $x > 0.1-0.25$ the solid solution is single-phase with the vaterite structure (space group $C2/c$). It should be noted that $Lu_{1-x}Gd_xBO_3$ orthoborates at $x \ge 0.12$ have the vaterite structure, while the vaterite structure in $Lu_{1-x}Re_xBO_3$ compounds (Re = Eu, Tb, Dy) appears only at $x \ge 0.2$, and in $Lu_{1-x}Y_xBO_3$ — at $x \ge 0.25$.

The $La_{0.98-x}Lu_xEu_{0.02}BO_3$ solid solution, synthesized at $T = 970$°C (the temperature of presence of the $LaBO_3$ aragonite and the $LuBO_3$ calcite phase) was studied in [9]. Instead of the anticipated phase sequence with increase of x: aragonite → aragonite + calcite → calcite, we experimentally observe a more complex sequence of structural states. As lutetium concentration increases, three types of crystalline phases change successively: aragonite, vaterite and calcite. The sequence of structural states in $La_{0.98-x}Lu_xEu_{0.02}BO_3$ compounds with an increase of Lu^{3+} concentration can be schematically represented as follows: aragonite (at $0 \le x < 0.15$) → aragonite + vaterite ($0.15 \le x \le 0.8$) → vaterite ($0.8 < x < 0.88$) → vaterite + calcite ($0.88 \le x < 0.93$) → calcite ($0.93 \le x \le 0.98$). The same sequence of structural state change is observed in $Pr_{0.99-x}Lu_xEu_{0.01}BO_3$ [27] orthoborates synthesized at $T = 970$°C (the temperature of presence of the $PrBO_3$ aragonite structure [22–24]). It should be noted that single-phase vaterite in $Pr_{0.99-x}Lu_xEu_{0.01}BO_3$ orthoborates forms in a wider range of Lu^{3+} concentrations ($0.6 < x \le 0.8$) than in $La_{0.98-x}Lu_xEu_{0.02}BO_3$ ($0.8 < x < 0.88$).

By changing the wavelength of light exciting the luminescence of optically active centers in a sample, for example Eu^{3+} centers, it is possible to obtain information about the structure of the near-surface layer and the volume of the sample [28–30]. When luminescence of Eu^{3+} ions in $LuBO_3$(Eu) orthoborates is excited by light which corresponds to the region of sample's intensive absorption, e.g., under band-to-band excitation, or in the charge transfer band (CTB) ($\lambda_{ex} = 225-275$ nm), information about the local environment of Eu^+ in the crystal near-surface layer can be obtained [1–3,28–33]. Under resonance excitation of luminescence of Eu^{3+} ions in the crystal transparency region ($\lambda_{ex} \sim 394$ and ~ 466 nm), we learn about the immediate environment of Eu^{3+} ions in the crystal bulk. A study of spectral characteristics of the near-surface layer and sample bulk has provided information about the structure on the surface and in the bulk of microcrystals in $Lu_{98-x}In_xEu_{0.02}BO_3$, $Lu_{0.99-x}Re_xEu_{0.01}BO_3$ (Re = Eu, Gd, Tb, Y) and $La_{0.98-x}Lu_xEu_{0.02}BO_3$ solid solutions [8,9,25,26].

Structural transformations in $Lu_{0.98-x}In_xEu_{0.02}BO_3$ orthoborates synthesized at 780°C (the temperature of presence of $LuBO_3$ vaterite), upon an increase of In^{3+} ion concentration, begin in the near-surface layer of the microcrystals of these samples. At $x \ge 0.04$ the near-surface layer has the calcite structure, with further increase of indium concentration the amount of the calcite phase also increases in the bulk of the sample microcrystals, while at $x > 0.1$ the whole sample has the calcite structure [8]. At the same time, the vaterite phase in the $Lu_{1-x}Gd_xBO_3$ orthoborate synthesized at 970°C (the temperature of presence of $LuBO_3$ calcite) forms at $x > 0.05$ in the bulk of large microcrystals having the calcite structure, and is also observed on their surface with a further increase of Gd^{3+} ion concentration [25,26]. With an increase of Lu^{3+} (x) concentration, the vaterite phase forms in the samples of $La_{0.98-x}Lu_xEu_{0.02}BO_3$, synthesized at 970°C (which initially have the aragonite structure), like in the samples of $Lu_{1-x}Re_xBO_3$, first in the bulk of sample microcrystals, and then the vaterite structure forms in the whole sample. At the same time, the calcite phase at $0.88 < x < 0.93$ in the $La_{0.98-x}Lu_xEu_{0.02}BO_3$ orthoborates, which have the vaterite structure, forms first in the near-surface regions of microcrystals, and then the calcite structure forms in the whole sample, like in the samples of $Lu_{0.98-x}In_xEu_{0.02}BO_3$ [9].

As already noted, the $LaBO_3$ ($PrBO_3$) orthoborates synthesized at 970°C have the aragonite structure, and $LuBO_3$ — the calcite structure. However, as already noted, first the vaterite phase forms in the solid solution

of $Re_{1-x}Lu_xBO_3$, $(Re = La, Pr)$ synthesized at 970°C (initially it has the aragonite structure), when concentration of Lu^{3+} increases, and only then, with a further increase of x, the $Re_{1-x}Lu_xBO_3$ compound becomes a calcite. Due to such structural changes of $Re_{1-x}Lu_xBO_3$, $(Re = La, Pr)$ solid solutions, it is reasonable to study a solid solution consisting of orthoborates having the aragonite and vaterite structure. Such orthoborates are $LaBO_3$ and YBO_3.

In the present paper we study the structural changes, morphology, IR spectra, as well as luminescence excitation spectra and luminescence spectra of $La_{0.99-x}Y_xEu_{0.01}BO_3$ solid solutions in a wide range of Y concentrations $(0 \le x \le 0.99)$. Eu^{3+} ions, like in our previous research, were used as optically active and structure-sensitive labels in amounts not affecting the structural transformations of orthoborates. The correspondence between structure and spectral characteristics of these compounds was established.

2. Experimental procedures

2.1. Sample synthesis

Samples of polycrystalline powders of $La_{0.99-x}Y_xEu_{0.01}BO_3$ orthoborates were obtained by interaction of oxides of rare earth elements with molten potassium tetraborate according to the reaction

$$(0.99 - x)La_2O_3 + xY_2O_3 + 0.01Eu_2O_3 + K_2B_4O_7 = 2La_{0.99-x}Y_xEu_{0.01}BO_3 + K_2B_2O_4.$$

The potassium tetraborate amount taken for the reaction provided a 10–20% excess of the boron-containing reagent in relation to the stoichiometric amount. The initial compounds for orthoborate synthesis were potassium tetraborate tetrahydrate $K_2B_4O_7 \cdot 4H_2O$ and calibrated aqueous solutions of nitrates of rare earth elements. All the used chemical substances were of „analytical reagent grade".

Microcrystalline orthoborate powders were synthesized as follows. A weighed amount of potassium tetraborate tetrahydrate was placed in a ceramic round-bottomed cup, stoichiometric amounts of aqueous solutions of rare earth nitrates, taken in the required ratio, were added and thoroughly mixed. The obtained aqueous suspension was heated on a hot plate and water was driven off under weak boiling. The obtained solid product was annealed at 550°C for 20 min to remove water and nitrate decomposition products, and then thoroughly ground in an agate mortar. The obtained powder was transferred into a ceramic crucible and subjected to high-temperature annealing at $T = 970$°C for 2 h. The annealing product was treated with aqueous solution of hydrochloric acid with the concentration of 5 wt.% for 0.2 h while constantly mixing on a magnetic mixer. Orthoborate polycrystals were isolated by filtering the obtained aqueous suspension, followed by washing with water, alcohol, and product drying on a filter. The obtained powders of orthoborate polycrystals were finally dried in air at $T = 200$°C for 0.5 h.

2.2. Research methods

X-ray diffraction studies were performed using a Rigaku SmartLab SE diffractometer with CuK_α-radiation, $\lambda = 1.54178$ Å, 40 kV, 35 mA. Angular interval was $2\theta = 10-140°$. Phase analysis of the samples and calculation of lattice parameters were performed using the Match and PowderCell 2.4 programs.

The IR absorption spectra of the samples were measured using a Fourier-spectrometer VERTEX 80v in the spectral range of $400-5000\,cm^{-1}$, resolution being $2\,cm^{-1}$. For measurements, the polycrystal powders were ground in an agate mortar, and then were applied in a thin layer onto a polished crystalline substrate of KBr.

The sample morphology was studied using a Supra 50VP X-ray microanalyzer with an add-on for EDS INCA (Oxford).

Photoluminescence spectra and luminescence excitation spectra were studied on a unit consisting of a light source — DKSSh-150 lamp, two MDR-4 and MDR-6 monochromators (spectral range 200–1000 nm, dispersion 1.3 nm/mm). Luminescence was recorded by means of a FEU-106 photomultiplier (spectral sensitivity region 200–800 nm) and an amplification system. The MDR-4 monochromator was used to study the samples' luminescence excitation spectra, the MDR-6 monochromator was used to study luminescence spectra.

Spectral and structural characteristics, as well as the sample morphology were studied at room temperature.

3. X-ray diffraction studies

The diffraction patterns of the powder samples of the studied $La_{0.99-x}Y_xEu_{0.01}BO_3$ compounds and their phase composition at $0 \le x \le 0.99$ are shown in Fig. 1 and 2.

When $LaBO_3$ is doped with Y^{3+} ions at $0 \le x \le 0.1$, the samples are single-phase and have the aragonite structure, space group $Pnam$ № 62 (PDF 12-0762), $Z = 4$. The samples are two-phase in the range of $0.1 < x \le 0.8$ — the vaterite phase is observed along with the aragonite structure. At $0.8 < x \le 0.99$ the samples are single-phase with the vaterite structure (space group $P6_3/m$ № 176). A decrease of the unit cell volume with an increase of x is observed in single-phase $La_{0.99-x}Y_xEu_{0.01}BO_3$ samples $(0 \le x \le 0.1)$ having the aragonite structure (Fig. 3). This means dissolution of yttrium in the aragonite structure, since the ionic radius of Y^{3+} (0.92836 Å) is smaller than the ionic radius of La^{3+} (1.11482 Å) [34]. In the two-phase region (aragonite + vaterite), the unit cell volume of each of these phases does not change, only a quantitative change of the aragonite and vaterite phase correlation takes place.

When $Y_{0.99}Eu_{0.01}BO_3$ is doped with La^{3+} ions having a larger ionic radius as compared to Y^{3+}, we observe an increase of the vaterite unit cell volume as the concentration of La^{3+} rises in single-phase $La_{0.99-x}Y_xEu_{0.01}BO_3$ samples at $0.99 \ge x \ge 0.8$, which means dissolution of La^{3+} in the vaterite structure (Fig. 3).

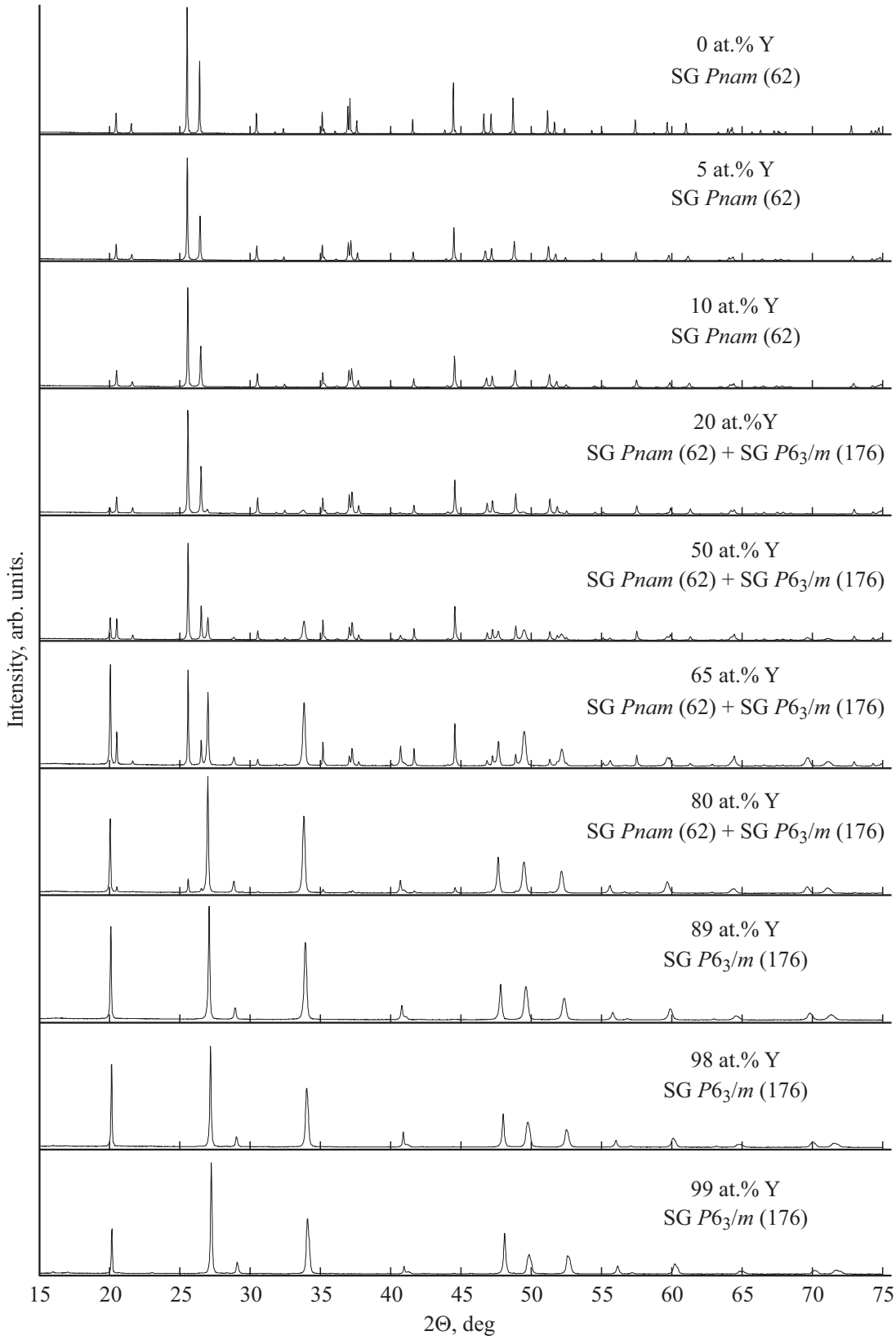

Figure 1. Diffraction patterns for samples of $La_{0.99-x}Y_xEu_{0.01}BO_3$ ($0 \leq x \leq 0.99$).

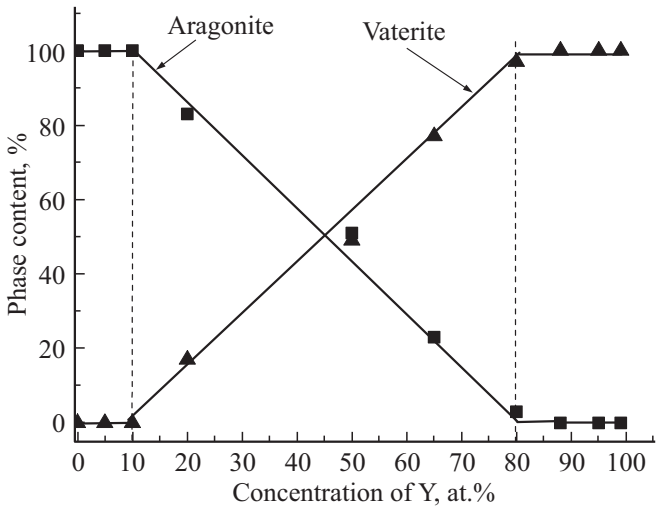

Figure 2. Phase composition of the synthesized samples of $La_{0.99-x}Y_xEu_{0.01}BO_3$ depending on rare earths ratio in the charge at $0 \le x \le 0.99$: a square means aragonite, a triangle means vaterite.

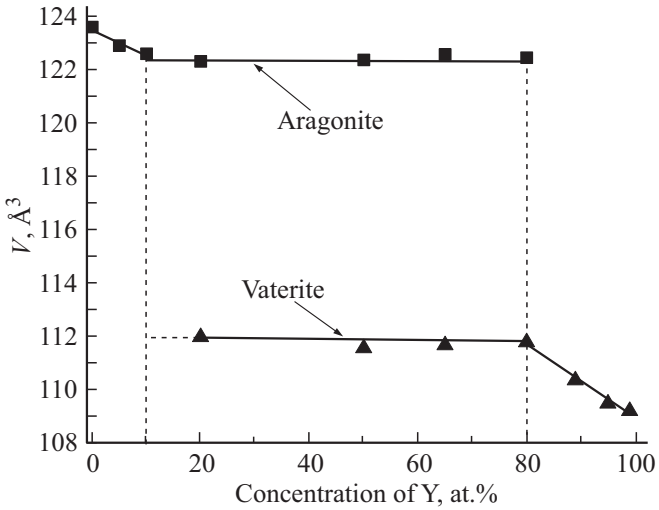

Figure 3. Volumes of unit cells of structural modifications of $La_{0.99-x}Y_xEu_{0.01}BO_3$ at $0 \le x \le 0.99$ reduced to $Z = 2$: a square means aragonite, a triangle means vaterite.

The maximum possible dissolution of Y^{3+} ions in the aragonite phase of $La_{0.99}Eu_{0.01}BO_3$ is ~ 10 at.%. The composition of the forming solid solution is $\sim La_{0.89}Y_{0.1}Eu_{0.01}BO_3$.

The approximate composition of the vaterite phase of $La_{0.99-x}Y_xEu_{0.01}BO_3$, determined along the boundary of change of the vaterite unit cell volume is $\sim La_{0.19}Y_{0.8}Eu_{0.01}BO_3$.

Thus, three regions of Y^{3+} concentrations, where certain structural states exist, can be distinguished in $La_{0.99-x}Y_xEu_{0.01}BO_3$ orthoborates. At $0 \le x \le 0.1$, the solid solution of $La_{0.99-x}Y_xEu_{0.01}BO_3$ has the aragonite structure, the samples are two-phase in the range of $0.1 < x \le 0.8$ — the vaterite phase is observed along with the aragonite structure, while at $0.8 < x \le 0.99$ the samples are single-phase with the vaterite structure (the Table).

Influence of Y^{3+} concentration on content of aragonite and vaterite phases in $La_{0.99-x}Y_xEu_{0.01}BO_3$ orthoborates

Concentration of Y^{3+}, at.%	Aragonite, %	V_A, Å^3	Vaterite, %	V_V, Å^3
0	100	123.57	0	
5	100	122.90	0	
10	100	122.60	0	
20	83	122.31	17	111.96
50	51	122.37	49	111.54
65	23	122.57	77	111.65
80	3	122.45	97	111.76
89	0		100	110.33
95	0		100	109.46
99	0		100	109.18

Note. V_A is volume of aragonite unit cell reduced to $Z = 2$. V_V is volume of vaterite unit cell, $Z = 2$.

4. Sample morphology

Microcrystals sized $\sim 1-3\,\mu$m (Fig. 4, *a*) are observed in the samples of $La_{0.99-x}Y_xEu_{0.01}BO_3$ in the Y^{3+} concentration range of $0 \le x \le 0.1$, which have the aragonite structure according to the X-ray diffraction analysis data (the Table). Microcrystals of the same sizes are observed in the samples of $La_{0.79}Y_{0.2}Eu_{0.01}BO_3$ which contain 23% of aragonite (A) and 77% of vaterite (V) (Fig. 4, *b*). The samples of $La_{0.49}Y_{0.5}Eu_{0.01}BO_3$ (51% A, 49% V) consist of microcrystals sized $0.5-6\,\mu$m. Cracks are observed in larger microcrystals in these samples (Fig. 4, *c*). The quantity of small crystals increases with a further increase of the concentration of Y^{3+}. $La_{0.19}Y_{0.8}Eu_{0.01}BO_3$ orthoborates (3% A, 93% V) consist both of microcrystals sized $0.5-1\,\mu$m and large microcrystals of $6-10\,\mu$m, which have many cracks (Fig. 4, *d*). The samples of $La_{0.1}Y_{0.89}Eu_{0.01}BO_3$ (100% V) have chiefly microcrystals sized $0.3-0.7\,\mu$m. These samples contain a small number of large crystals ($\sim 6\,\mu$m) where multiple cracks are observed (Fig. 4, *e*). The samples of $Y_{0.99}Eu_{0.01}BO_3$ (100% V) consist of microcrystals sized $1-6\,\mu$m. Discontinuities in the form of cracks are observed in large microcrystals (Fig. 4, *f*).

Thus, microcrystals sized $1-3\,\mu$m are observed in the samples of $La_{0.99-x}Y_xEu_{0.01}BO_3$ having the aragonite structure, like in the $La_{0.98-x}Re_xEu_{0.02}BO_3$ compounds ($Re = Lu, Pr$) [9,27]. Microcrystals sized $1-6\,\mu$m, which have discontinuities in the form of cracks, are observed in the $Y_{0.99}Eu_{0.01}BO_3$ compounds with the vaterite struc-

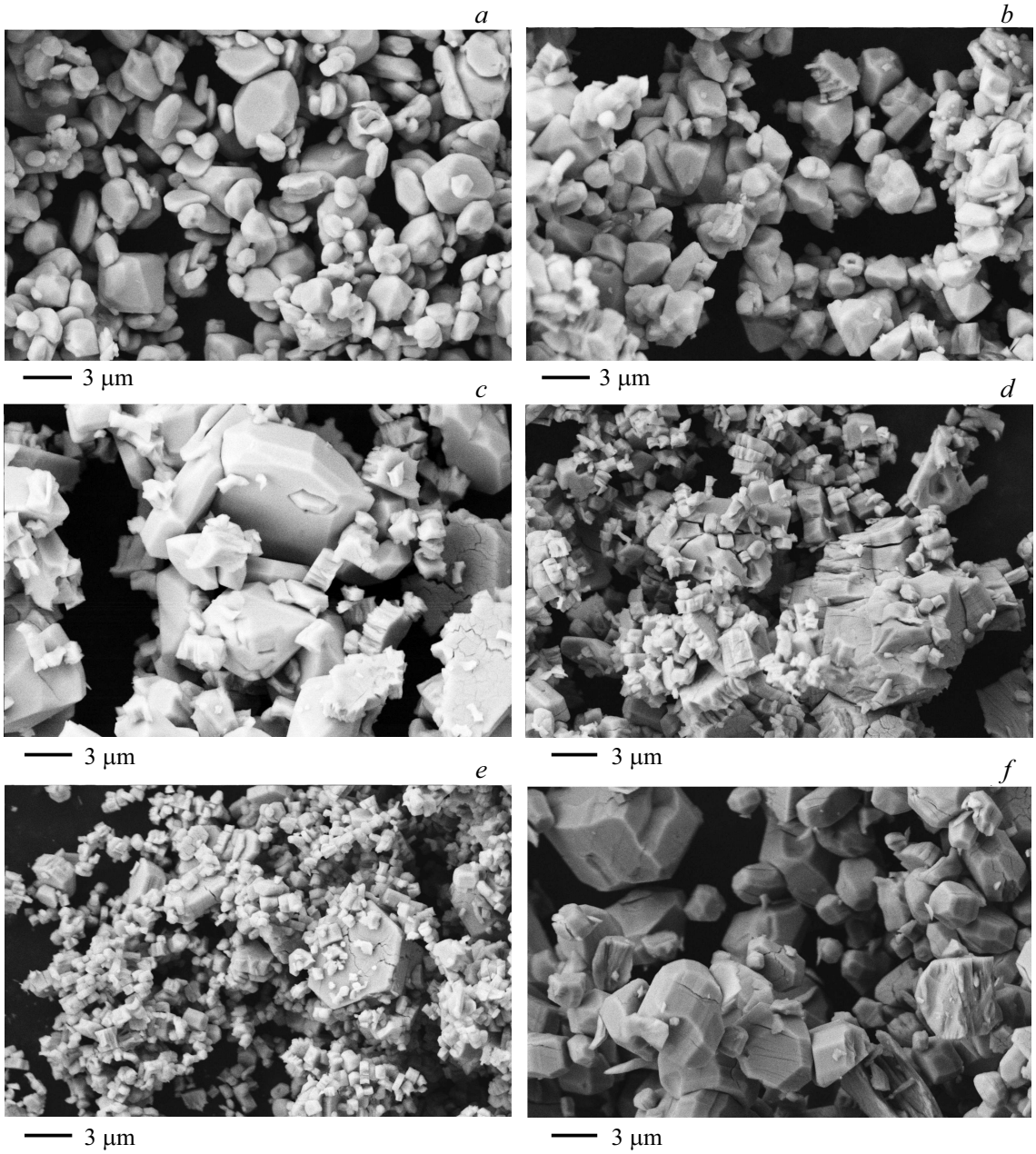

Figure 4. Morphology of the samples of $La_{0.99-x}Y_xEu_{0.01}BO_3$. *a* — $La_{0.89}Y_{0.1}Eu_{0.01}BO_3$; *b* — $La_{0.79}Y_{0.2}Eu_{0.01}BO_3$; *c* — $La_{0.49}Y_{0.5}Eu_{0.01}BO_3$; *d* — $La_{0.19}Y_{0.8}Eu_{0.01}BO_3$; *e* — $La_{0.1}Y_{0.89}Eu_{0.01}BO_3$; *f* — $Y_{0.99}Eu_{0.01}BO_3$.

ture. The number of small crystals increases in the samples of $La_{0.99-x}Y_xEu_{0.01}BO_3$ at $x > 0.1$ with an increase of vaterite amount. The $La_{0.1}Y_{0.89}Eu_{0.01}BO_3$ compound (100% V) have chiefly microcrystals sized $0.3-0.7\,\mu$m.

5. Results of IR spectroscopy

Fig. 5 shows the IR spectra of the samples of the studied $La_{0.99-x}Y_xEu_{0.01}BO_3$ compounds at $0 \le x \le 0.99$ in the frequency range of internal vibrations of the B–O bonds. The spectrum of the sample consisting of $La_{0.98}Eu_{0.02}BO_3$ (Fig. 5, spectrum *1*) has absorption bands 592, 612, 721, 739, 939 and 1302 cm^{-1}. According to the X-ray diffraction analysis data, the synthesized $La_{0.98}Eu_{0.02}BO_3$ crystallizes in the aragonite lattice (the Table).

Each boron atom in the aragonite structure is surrounded by three oxygen atoms. The IR spectra of $LaBO_3$ and their analysis are given in several papers [23,35,36]. A comparison of the IR spectra of the $La_{0.98}Eu_{0.02}BO_3$ compound (Fig. 5, spectrum *1*) with the published data for $LaBO_3$ shows that the observed absorption bands are typical for the aragonite structure. The IR spectrum for the $La_{0.89}Y_{0.1}Eu_{0.01}BO_3$ compound (Fig. 5, spectrum *2*), which also has the aragonite structure (the Table), is the same as

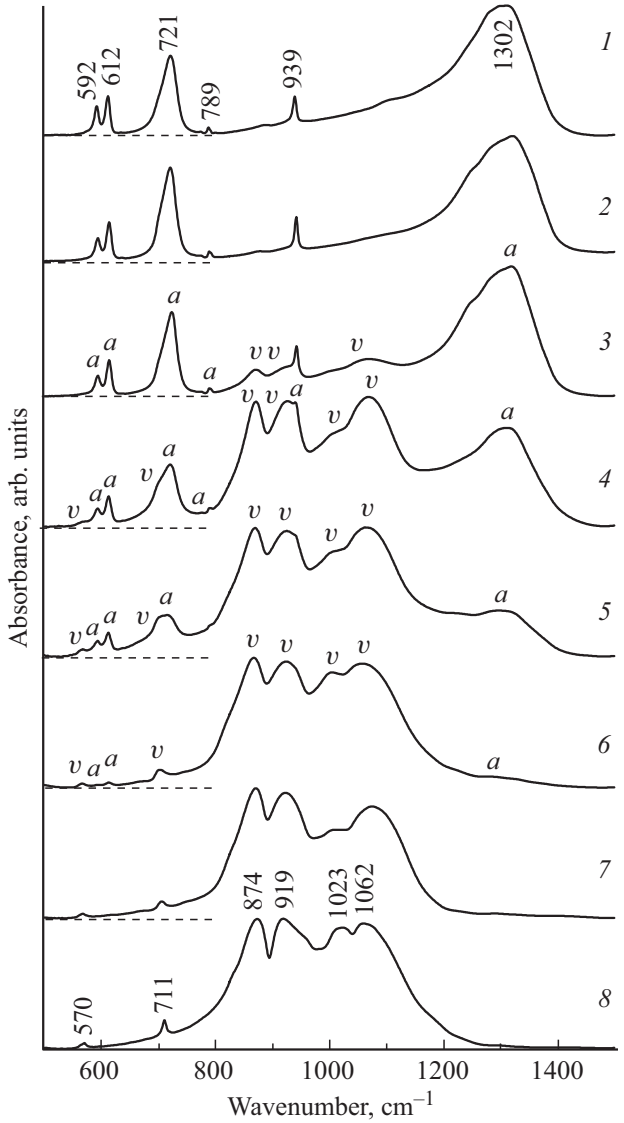

Figure 5. IR spectra of $La_{0.99-x}Y_xEu_{0.01}BO_3$ orthoborates. *1* — $La_{0.98}Eu_{0.02}BO_3$; *2* — $La_{0.89}Y_{0.1}Eu_{0.01}BO_3$; *3* — $La_{0.79}Y_{0.2}Eu_{0.01}BO_3$; *4* — $La_{0.49}Y_{0.5}Eu_{0.01}BO_3$; *5* — $La_{0.34}Y_{0.65}Eu_{0.01}BO_3$; *6* — $La_{0.19}Y_{0.8}Eu_{0.01}BO_3$; *7* — $La_{0.1}Y_{0.89}Eu_{0.01}BO_3$; *8* — $Y_{0.99}Eu_{0.01}BO_3$. The zero values of ordinate axes for the spectra *1–7* are shown with a thin dashed line.

for $La_{0.98}Eu_{0.02}BO_3$ orthoborate. With a further increase of the concentration of Y^{3+} ions, additional bands marked „v" are observed in the spectra of the $La_{0.99-x}Y_xEu_{0.01}BO_3$ samples in the range of $0.1 < x \leq 0.8$. According to the X-ray diffraction analysis results, these samples are two-phase and contain the aragonite and vaterite phases (the Table). Intensity of the bands „v" in the spectrum of the $La_{0.79}Y_{0.2}Eu_{0.01}BO_3$ compound is insignificant as compared to the aragonite phase bands „a". The sample contains 73% of the aragonite phase and 17% of the vaterite phase. With an increase of Y^{3+} ion concentration, intensity of the IR absorption bands, typical for the aragonite phase „a", decreases, while that of the bands, corresponding to the vaterite structure „v", increases (Fig. 5, spectra *3–6*). It should be noted that the share of the vaterite phase in the $La_{0.19}Y_{0.8}Eu_{0.01}BO_3$ sample is 97%, while that of aragonite is only 3%, and, nevertheless, very weak bands of 592, 612 and 1302 cm^{-1}, typical for the aragonite phase („a"), are present in the IR spectrum of this sample (Fig. 5, spectrum *6*). The samples of $La_{0.1}Y_{0.89}Eu_{0.01}BO_3$ and $Y_{0.99}Eu_{0.01}BO_3$ (Fig. 5, spectra *7, 8*) as per the X-ray diffraction analysis data, are single-phase with the vaterite structure. The IR spectra of these samples have the absorption bands of 570, 711, 874, 919, 1023, 1062 cm^{-1}, typical for the spectra of the rare earth element orthoborates and yttrium borate with the vaterite structure [5,23,37,38].

Boron ions in the aragonite structure have trigonal coordination by oxygen — $(BO_3)^{3-}$, but three boron atoms with tetrahedral environment by oxygen in the vaterite structure make up a group $(B_3O_9)^{9-}$ in the form of a three-dimensional ring. The bands in the frequency range of 800–1200 cm^{-1} are due to stretching vibrations B–O-bonds of the ring and terminal bonds B–O (Fig. 5, spectra *7, 8*).

Thus, we observe a correspondence between the structural modification and the IR absorption spectrum of $La_{0.99-x}Y_xEu_{0.01}BO_3$ orthoborates in the range of $0 \leq x \leq 0.99$. At $0 \leq x \leq 0.1$ and $0.8 < x \leq 0.99$, the IR spectra of these compounds have the bands typical only for the aragonite and vaterite structures respectively. The IR spectra at $0.1 < x \leq 0.8$ contain the bands corresponding both to the aragonite and vaterite structures.

6. Luminescence spectra and luminescence excitation spectra of $La_{0.99-x}Y_xEu_{0.01}BO_3$

The luminescence spectra (LS) and luminescence excitation spectra (LES) of the main luminescence bands of $La_{0.99-x}Y_xEu_{0.01}BO_3$ orthoborates ($0 \leq x \leq 0.99$) for different structural modifications of these compounds (aragonite, aragonite + vaterite, vaterite) are shown in Fig. 6–8.

6.1. Luminescence excitation spectra

The luminescence excitation spectrum (LES) of the most intense luminescence band of the $La_{0.94}Y_{0.05}Eu_{0.01}BO_3$ orthoborate ($\lambda_{max} = 614.5$ nm ($^5D_0 \rightarrow {}^7F_2$)) is shown in Fig. 6, spectrum *1*. The most intense band in the LES is the wide band ($\lambda = 230–340$ nm) in the ultraviolet spectrum region with the maximum at $\lambda_{ex} \sim 278$ nm (charge transfer band — CTB). The LES also contains several narrow bands in the wavelength range of 290–500 nm, corresponding to resonance excitation of Eu^{3+} ions. The most intense bands in the long wavelength spectrum range are the bands corresponding to resonance excitation of Eu^{3+} ions ($\lambda_{ex} = 393.75$ nm ($^7F_0 \rightarrow {}^5L_6$) and 465.5 nm ($^7F_0 \rightarrow {}^5D_2$)) (Fig. 6, spectrum *1*, Fig. 7, spectrum *1*). Similar spectra

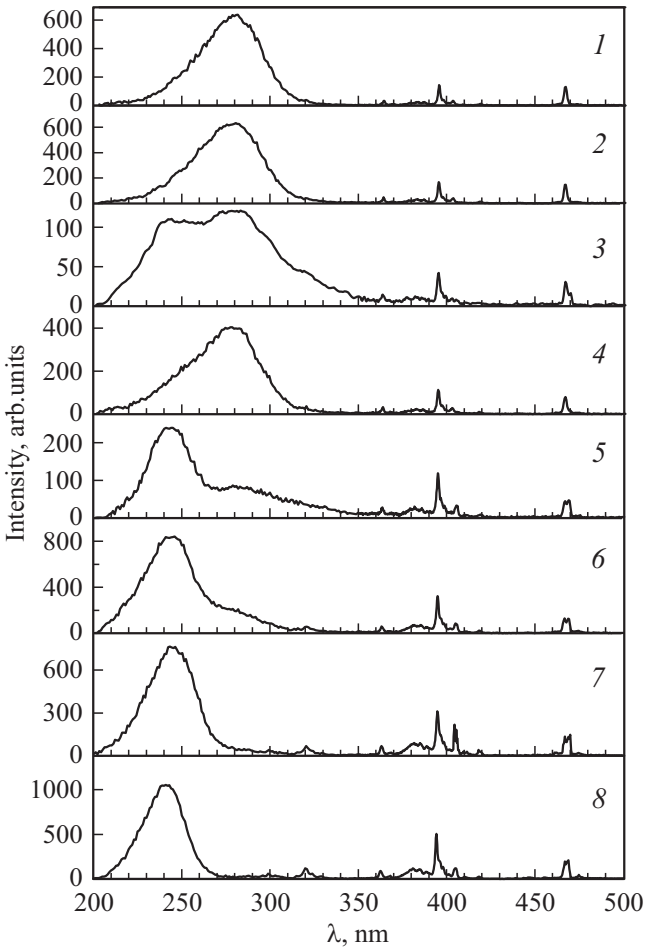

Figure 6. Luminescence excitation spectra of $La_{0.99-x}Y_xEu_{0.01}BO_3$ orthoborates. *1* — $La_{0.94}Y_{0.05}Eu_{0.01}BO_3$; *2* — $La_{0.79}Y_{0.2}Eu_{0.01}BO_3$; *3* — $La_{0.79}Y_{0.2}Eu_{0.01}BO_3$; *4* — $La_{0.49}Y_{0.5}Eu_{0.01}BO_3$; *5* — $La_{0.49}Y_{0.5}Eu_{0.01}BO_3$; *6* — $La_{0.34}Y_{0.65}Eu_{0.01}BO_3$; *7* — $La_{0.19}Y_{0.8}Eu_{0.01}BO_3$; *8* — $Y_{0.99}Eu_{0.01}BO_3$. *1, 2, 4* — $\lambda_{max} = 614.5$ nm; *3, 5* — $\lambda_{max} = 627$ nm; *6, 7, 8* — $\lambda_{max} = 592.6$ nm.

are observed for the samples of $La_{0.99-x}Y_xEu_{0.01}BO_3$ at $0 \le x \le 0.2$. As an example, Fig. 6, spectrum *2* shows the LES-bands of luminescence with $\lambda_{max} = 614.5$ nm of the $La_{0.79}Y_{0.2}Eu_{0.01}BO_3$ orthoborate that contains 83% of aragonite (A) and 17% of vaterite (V) (the Table). The luminescence spectrum of the $La_{0.49}Y_{0.5}Eu_{0.01}BO_3$ sample (51% A, 41% V) has, along with the bands corresponding to the aragonite structure, the band ($\lambda_{max} \sim 627$ nm ($^5D_0 \rightarrow {}^7F_2$)) typical for the vaterite phase; this band does not overlap with the bands corresponding to the aragonite phase (Fig. 8, spectrum *6*). Fig. 6, spectra *4, 5*, shows the luminescence excitation spectra of luminescence bands with $\lambda_{max} = 614.5$ and 627 nm for $La_{0.49}Y_{0.5}Eu_{0.01}BO_3$ orthoborate. These spectra have considerable differences. The LES of the band with $\lambda_{max} = 614.5$ nm are the same as the spectra for the aragonite phase (Fig. 6, spectra *1, 2*). At the same time, the most intense band in the LES of luminescence with $\lambda_{max} = 627$ nm is the band with the maximum at $\lambda_{ex} = 242$ nm. The long wavelength edge of this band has a leg with the maximum at ~ 280 nm. Moreover, the LES of this sample contains the resonance bands of $\lambda_{ex} = 394.25$ and 466.5 nm, as well as one more band ($\lambda_{ex} = 469$ nm ($^7F_0 \rightarrow {}^5D_2$)), which corresponds to resonance excitation of Eu^{3+} ions (Fig. 6, spectrum *5*, Fig. 7, spectrum *5*). It should be noted that the ultraviolet band with the maximum at $\lambda_{ex} \sim 242$ nm in the LES is typical for the vaterite modification $ReBO_3(Eu)$ (Re = Eu, Tb, Lu, Gd, Y) [1–3,9–12]. The most intense band in the luminescence excitation spectrum of the most intense luminescence band ($\lambda_{max} = 592.6$ nm) for the $La_{0.34}Y_{0.65}Eu_{0.01}BO_3$ samples, containing 23% of aragonite and 77% of vaterite (the Table), is the band with the maximum at $\lambda_{ex} \sim 242$ nm. The LES of these samples also contains the band of $\lambda_{ex} = 469$ nm (Fig. 6, spectrum *6*, Fig. 7, spectrum *6*). The most intense band in the LES of $La_{0.99-x}Y_xEu_{0.01}BO_3$ orthoborates at $0.65 \le x \le 0.99$ is the band of 242–243 nm. These samples also have the resonance bands of 394.25, 466.5 and 469 nm (Fig. 6, 7, spectra *6–8*).

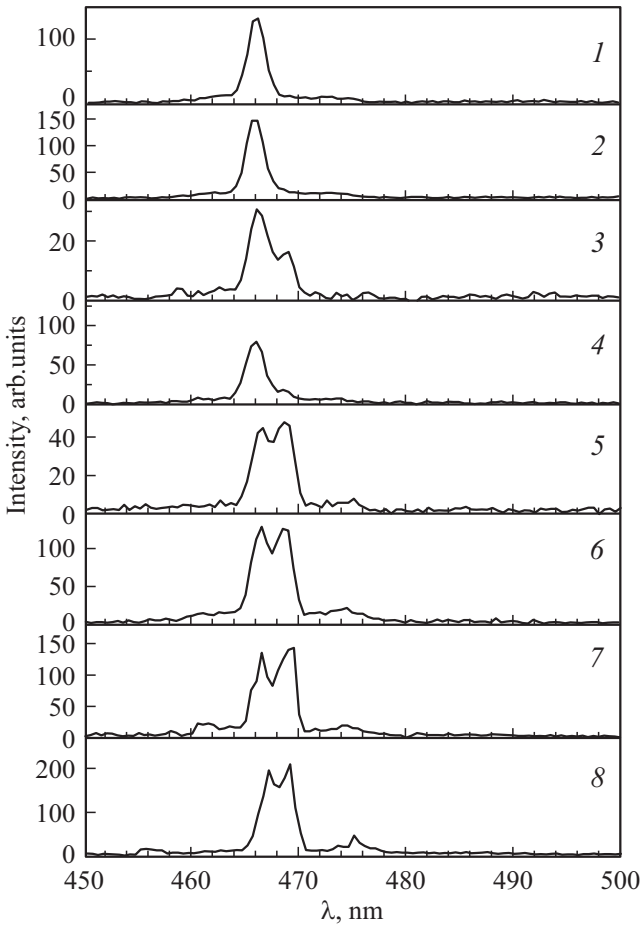

Figure 7. Luminescence excitation spectra of $La_{0.99-x}Y_xEu_{0.01}BO_3$ orthoborates, shown in Fig. 6, in the wavelength range of 450–500 nm.

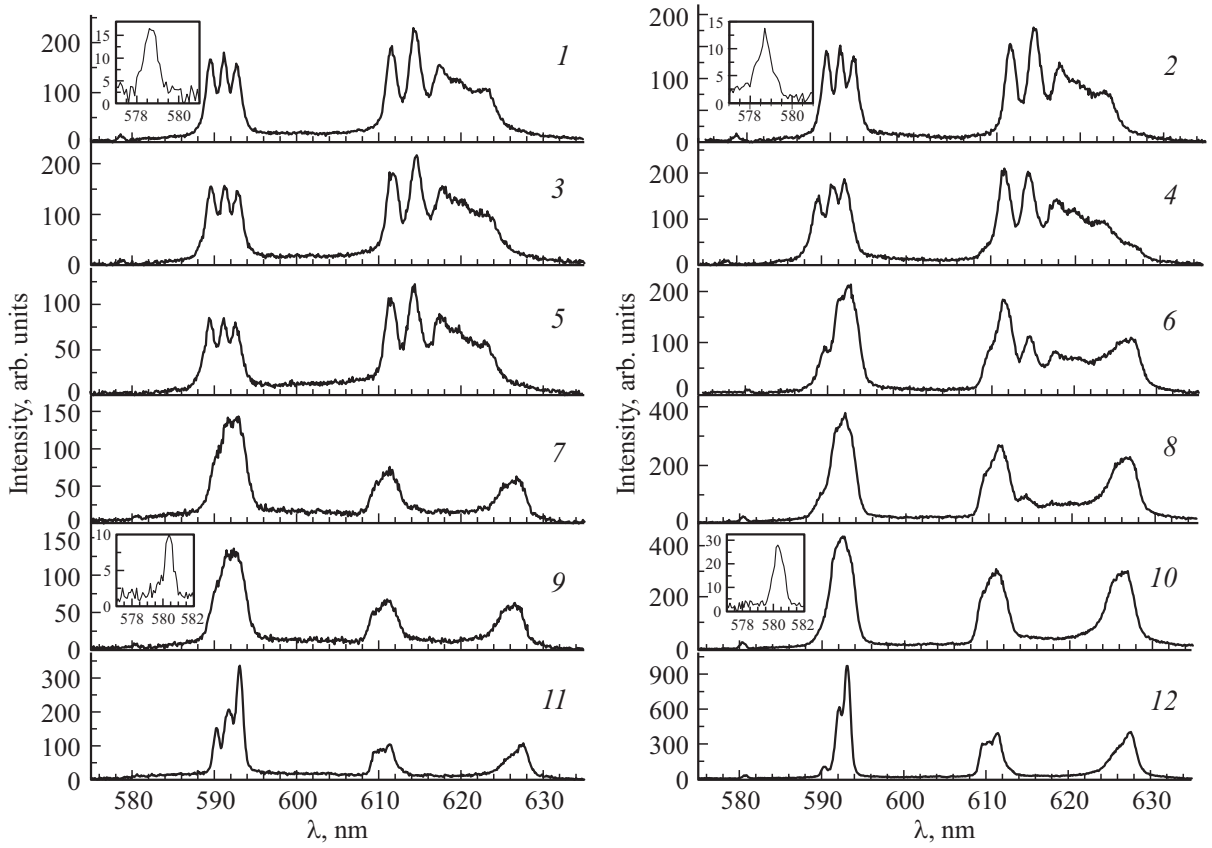

Figure 8. Luminescence spectra of $La_{0.99-x}Y_xEu_{0.01}BO_3$ orthoborates. *1, 2* — $La_{0.94}Y_{0.05}Eu_{0.01}BO_3$; *3, 4* — $La_{0.79}Y_{0.2}Eu_{0.01}BO_3$; *5, 6* — $La_{0.49}Y_{0.5}Eu_{0.01}BO_3$; *7, 8* — $La_{0.34}Y_{0.65}Eu_{0.01}BO_3$; *9, 10* — $La_{0.19}Y_{0.8}Eu_{0.01}BO_3$; *11, 12* — $Y_{0.99}Eu_{0.01}BO_3$. *1, 3, 5* — $\lambda_{ex} = 278$ nm; *7, 9* — $\lambda_{ex} = 243$ nm; *11* — $\lambda_{ex} = 242$ nm; *2, 4, 6, 8, 10, 12* — $\lambda_{ex} = 394$ nm. The insets show the luminescence spectra in the wavelength ranges of $\sim 576-582$ nm in scales enlarged along the axes of abscissa and ordinates.

Thus, the excitation spectrum of the main bands of luminescence of Eu^{3+} ions in the $La_{0.99-x}Y_xEu_{0.01}BO_3$ samples, containing 0–20 at.% Y, has the bands typical for the aragonite structure: the band with $\lambda_{ex} \sim 278$ nm (CTB) and the resonance bands of 393.75 and 465.5 nm. The LES of these compounds at the concentration of Y = 65–99 at.% contain the bands which are typical for the vaterite structure: the band with $\lambda_{ex} = 242-243$ nm (CTB) and the resonance bands of 394.25, 466.5 and 469 nm. It should be noted that if the positions of the maxima of the resonance bands of Eu^{3+} ion excitation (at $\lambda_{ex} \sim 394$ and 466 nm) are close in the LES of $La_{0.99-x}Y_xEu_{0.01}BO_3$ compounds, having aragonite and vaterite structures, then the positions of the maxima of the charge transfer bands (CTB) differ significantly.

It should be noted that the luminescence excitation spectra of the bands, typical for the vaterite modification $YBO_3(Eu)$, has a band of $\lambda_{ex} = 469$ nm which is not present in the LES of the bands typical for the $LaBO_3(Eu)$ compound having the aragonite structure. Therefore, presence or absence of the band with $\lambda_{ex} = 469$ nm in the LES can indicate the structural state of $La_{0.99-x}Y_xEu_{0.01}BO_3$ orthoborates.

6.2. Luminescence spectra

Fig. 8 shows the luminescence spectra (LS) of $La_{0.99-x}Y_xEu_{0.01}BO_3$ compounds ($0 \le x \le 0.99$) in the spectral range of 575–635 nm under excitation by light in the maximum of the charge transfer band ($\lambda_{ex} \sim 278-242$ nm) and under resonance excitation of Eu^{3+} ions ($\lambda_{ex} = 394$ nm). The LS of these samples which have the aragonite structure at $0 \le x \le 0.1$ (the Table) are identical. Fig. 8, spectra *1, 2*, shows the LS of $La_{0.94}Y_{0.05}Eu_{0.01}BO_3$ orthoborate as an example. The luminescence spectra of the near-surface layer ($\lambda_{ex} = 278$ nm) and the bulk ($\lambda_{ex} = 394$ nm) of this sample are the same. They contain bands with $\lambda_{max} = 578.6$ nm ($^5D_0 \rightarrow {}^7F_0$), 589.4, 591 and 592.6 nm ($^5D_0 \rightarrow {}^7F_1$), as well as bands of 611.6, 614.5, 617.4, 619.8 and 623 nm ($^5D_0 \rightarrow {}^7F_2$). We have previously observed the same bands in the luminescence spectra of $La_{0.98}Eu_{0.02}BO_3$ orthoborate which has the aragonite structure [9]. The LS of the near-surface layer in the $La_{0.79}Y_{0.2}Eu_{0.01}BO_3$ samples, which contain 83% of aragonite (A) and 27% of vaterite (V), features the bands typical for the aragonite structure $LaBO_3(Eu)$ (Fig. 8, spectrum *3*). At the same time, the luminescence spectrum of the bulk of this sample ($\lambda_{ex} = 394$ nm) has changes in the

correlation of intensities of the bands with $\lambda_{max} = 589.4$, 591 and 592.6 nm (Fig. 8, spectrum *4*). Moreover, a leg ($\lambda_{max} \sim 627$ nm) forms on the long-wavelength dip of the 623 nm band, along with the bands typical for the aragonite structure. The luminescence excitation spectrum of this band (Fig. 6, spectrum *3*) has, along with the band which is typical for the aragonite structure ($\lambda_{ex} \sim 278$ nm), a band with the maximum at $\lambda_{ex} \sim 242$ nm which is typical for the vaterite structure. It should be noted that the LES of luminescence with $\lambda_{max} \sim 627$ nm has a band with $\lambda_{ex} = 369$ nm, which is also typical for the vaterite structure (Fig. 7, spectrum *3*). The given data makes it possible to conclude that the vaterite phase forms in the $La_{0.99-x}Y_xEu_{0.01}BO_3$ samples in the bulk of microcrystals which have the aragonite structure, the same as in $La_{0.98-x}Lu_xEu_{0.02}BO_3$ orthoborates [9]. Still greater changes in the LS of the sample bulk ($\lambda_{ex} = 394$ nm) are observed in $La_{0.49}Y_{0.5}Eu_{0.01}BO_3$ compounds (51% A, 45% V). These samples have an increased intensity of the ~ 627 nm band, and there are also considerable changes in the wavelength region of 588–596 nm: the band with $\lambda_{max} \sim 592.6$ nm becomes the most intense (Fig. 8, curve *6*). At the same time, only the bands typical for the aragonite structure are observed in the luminescence spectrum of the near-surface layer ($\lambda_{ex} = 278$ nm) (Fig. 8, spectrum *5*). It should be noted that the most intense band in the luminescence excitation spectrum with $\lambda_{max} \sim 627$ nm is the band with $\lambda_{ex} \sim 242$ nm, typical for the vaterite structure (Fig. 6, spectrum *5*).

The luminescence spectra of the near-surface layer of microcrystals ($\lambda_{ex} \sim 242$ nm) and their bulk ($\lambda_{ex} = 394$ nm) for the $La_{0.34}Y_{0.65}Eu_{0.01}BO_3$ orthoborate (23% A and 77% V) mainly have the bands which are typical for the vaterite modification of YBO_3(Eu) compounds (Fig. 8, spectra *7, 8*). The most intense band in the luminescence excitation spectrum of the most intense luminescence band of the $La_{0.34}Y_{0.65}Eu_{0.01}BO_3$ samples ($\lambda_{max} = 592.6$ nm) is the band with $\lambda_{ex} \sim 242$ nm (Fig. 6, spectrum *6*). The luminescence spectra of the near-surface layer and bulk of the microcrystals of the $La_{0.19}Y_{0.8}Eu_{0.01}BO_3$ samples (3% A and 97% V) and $Y_{0.99}Eu_{0.01}BO_3$ samples (100% V), as well as LES of these compounds, contain only the bands which are typical for the vaterite modification of $LuBO_3$(Eu) compounds (Fig. 8, spectra *9–12*, Fig. 6, spectra *7, 8*).

Special attention should be paid to the spectral position of a band, corresponding to the $^5D_0 \rightarrow {}^7F_0$ electron transition, in the luminescence spectra; this band is weak but does not overlap with the other bands. The maximum of the said band in the samples which have the aragonite structure is located at $\lambda_{max} = 578.6$ nm (Fig. 8, spectra*1–4*). The maximum of the said band in the compounds which have the vaterite structure is located at 580.4 nm (Fig. 8, spectra *9–12*). That's why the band, which corresponds to the $^5D_0 \rightarrow {}^7F_0$ electron transition, can be an indicator of the sample's structural state, the same as the band of $\lambda_{ex} = 469$ nm in LES. If λ_{max} is less than 580 nm, the sample has the aragonite structure, if λ_{max} is more than 580 nm, the sample has the vaterite structure.

A comparison of the results of X-ray diffraction analysis and spectral studies makes it possible to conclude that there is a correspondence between the structure and spectral characteristics of $La_{0.99-x}Y_xEu_{0.01}BO_3$ orthoborates. Increase of x results in a successive change of various structural modifications. At $0 \leq x \leq 0.1$, the compound has the aragonite structure and the LES and LS have the bands which correspond to the aragonite structure (Fig. 6, spectrum *1*, Fig. 8, spectra *1, 2*). At $0.1 < x < 0.8$, the samples are two-phase and contain the aragonite and vaterite phases, and the spectra of these samples contain the bands of the aragonite and vaterite modifications (Fig. 6, spectra *5, 6*, Fig. 8, spectra *5–8*). At $0.8 < x \leq 0.99$, the orthoborates have the vaterite structure and the LES and LS contain bands of the vaterite modification (Fig. 6, spectra *7, 8*, Fig. 8, spectra *9–12*).

It should be noted that the vaterite phase forms in $La_{0.99-x}Y_xEu_{0.01}BO_3$ orthoborates, which have the aragonite structure, at $x > 0.1$ first in the bulk of microcrystals of these samples. With a further increase of Lu^{3+} ion concentration, the vaterite phase also forms on the sample surface. This process is similar to the formation of the vaterite phase in the bulk of $Lu_{0.98-x}Lu_xEu_{0.02}BO_3$ orthoborate at $x \geq 0.15$ [9].

7. Conclusion

In the present paper we have studied the structure, morphology, IR spectra, as well as luminescence excitation spectra and luminescence spectra of the near-surface layer and bulk of $La_{0.99-x}Y_xEu_{0.01}BO_3$ orthoborates, synthesized at 970°C, at $0 \leq x \leq 0.99$. An unambiguous correspondence between the structure and spectral characteristics of these compounds was established.

It was demonstrated that an increase of Y^{3+} ion concentration in $La_{0.99-x}Y_xEu_{0.01}BO_3$ orthoborates results in a successive change of their structural state and spectral characteristics:

– at $0 \leq x \leq 0.1$, the compounds are single-phase and have the aragonite structure (space group *Pnam*). The luminescence spectra (corresponding to the aragonite structure) of Eu^{3+} ions in the near-surface layer and bulk of microcrystals of these samples contain, like in the $La_{0.98-x}Lu_xEu_{0.02}BO_3$ compounds, the bands with $\lambda_{max} = 589.4$, 591 and 592.6 nm, which correspond to the $^5D_0 \rightarrow {}^7F_1$ electron transition, as well as the bands of 611.6, 614.5, 617.4, 619.8, 621.3 and 623 nm ($^5D_0 \rightarrow {}^7F_2$). The luminescence excitation spectrum has a band of $\lambda_{ex} \sim 278$ nm (charge transfer band — CTB), as well as the bands which correspond to resonance excitation of Eu^{3+} ions ($\lambda_{ex} = 394$ nm ($^7F_0 \rightarrow {}^5L_6$) and 466.5 nm ($^7F_0 \rightarrow {}^5D_2$)). The IR spectra contain the absorption bands of 592, 612, 721, 789, 939 and 1302 cm^{-1} which are typical for the aragonite phase;

– at $0.1 < x < 0.8$, the $La_{0.99-x}Y_xEu_{0.01}BO_3$ samples are two-phase and contain the aragonite and vaterite phases. The luminescence and IR spectra of these samples contain the bands which are typical for the aragonite $La_{0.99}Eu_{0.01}BO_3$ and vaterite structures $Y_{0.99}Eu_{0.01}BO_3$;

– at $0.8 < x \leq 0.99$, the orthoborates have the vaterite structure (space group $P6_3/m$). The luminescence spectra of Eu^{3+} ions in the near-surface layer and the bulk of microcrystals of these samples are identical and contain the bands of 588–596, 608–613 and 624–632 nm which are typical for $Y_{0.99}Eu_{0.01}BO_3$. The LES has a band with $\lambda_{ex} \sim 242$ nm (charge transfer band — CTB), as well as the resonance bands of 394, 466.5 and 469 nm. The IR spectra of the vaterite contain the absorption bands of 570, 711, 874, 919, 1023 and 1062 cm^{-1}.

It has been established that the vaterite phase forms in the $La_{0.99-x}Y_xEu_{0.01}BO_3$ samples (initially having the aragonite structure) with an increase of Y^{3+} ion concentration, first in the bulk of sample microcrystals, and then in the whole sample.

It has been demonstrated for the first time that the band with $\lambda_{ex} = 369$ nm ($^7F_0 \rightarrow {}^5D_2$) in LES and the band in the wavelength region of 575–582 nm ($^5D_0 \rightarrow {}^7F_0$) in LS of $La_{0.99-x}Y_xEu_{0.01}BO_3$ compounds can be used as indicators of sample's structural state. The LES of the samples having the vaterite phase contain the band with $\lambda_{ex} = 369$ nm, while this band is not present in the samples having the aragonite structure. If in the SL the maximum of the band, which corresponds to the $^5D_0 \rightarrow {}^7F_0$ transition, is located at wavelengths shorter than 580 nm, the sample has the aragonite structure, if at λ longer than 580 nm, the sample has the vaterite structure.

Acknowledgments

The authors thank the Research Facility Center of ISSP RAS for the study of the sample morphology and their characterization by IR spectroscopy and X-ray diffraction analysis methods.

Funding

The work has been performed under the state assignment of ISSP of RAS.

Conflict of interest

The authors declare that they have no conflict of interest.

References

[1] C. Mansuy, J.M. Nedelec, C. Dujardin, R. Mahiou. Opt. Mater. **29**, *6*, 697 (2007).
[2] G. Blasse, B.C. Grabmaier. Luminescent Materials. Springer–Verlag (1994). 233 p.
[3] Jun Yang, Chunxia Li, Xiaoming Zhang, Zewei Quan, Cuimiao Zhang, Huaiyong Li, Jun Lin. Chem. Eur. J. **14**, *14*, 4336 (2008).
[4] S.Z. Shmurak, V.V. Kedrov, A.P. Kiselev, I.M. Shmyt'ko. FTT **57**, *1*, 19 (2015) (in Russian).
[5] S.Z. Shmurak, V.V. Kedrov, A.P. Kiselev, T.N. Fursova, I.M. Shmyt'ko. FTT **57**, *8*, 1558 (2015) (in Russian).
[6] Wen Ding, Pan Liang, Zhi-Hong Liu. Mater. Res. Bull. **94**, 31 (2017).
[7] Wen Ding, Pan Liang, Zhi-Hong Liu. Solid State Sci. **67**, 76 (2017).
[8] S.Z. Shmurak, V.V. Kedrov, A.P. Kiselev, T.N. Fursova, I.I. Zver'kova. FTT **62**, *12*, 2110 (2020) (in Russian).
[9] S.Z. Shmurak, V.V. Kedrov, A.P. Kiselev, T.N. Fursova, I.I. Zverkova, S.S. Khasanov. FTT **63**, *12*, 2142 (2021) (in Russian).
[10] N.I. Steblevskaya, M.I. Belobeletskaya, M.A. Medkov. Zhurn. neorgan. khimii **66**, *4*, 440 (2021) (in Russian).
[11] J. Guang, C. Zhang, C. Wang, L. Liu, C. Huang, S. Ding. Cryst. Eng. Commun. **14**, 579 (2012).
[12] J. Zhang, M. Yang, H Jin, X. Wang, X. Zhao, X. Liu, L. Peng. Mater. Res. Bull. **47**, 247 (2012).
[13] E.M. Levin, R.S. Roth, J.B. Martin. Am. Miner. **46**, *9–10*, 1030 (1961).
[14] J. Hölsä. Inorg. Chim. Acta **139**, *1–2*, 257 (1987).
[15] G. Chadeyron, M. El-Ghozzi, R. Mahiou, A. Arbus, C. Cousseins. J. Solid State Chem. **128**, 261 (1997).
[16] R.S. Roth, J.L. Waring, E.M. Levin. Proc. 3rd. Conf. Rare Earth Res. Clearwater, Fla (1964). P. 153.
[17] J. Zhang, M. Yang, H Jin, X. Wang, X. Zhao, X. Liu, L. Peng. Mater. Res. Bull. **47**, 247 (2012).
[18] I.M. Shmyt'ko, I.N. Kiryakin, G.K. Strukova. FTT **55**, *7*, 1369 (2013) (in Russian).
[19] Heng-Wei Wei, Li-Ming Shao, Huan Jiao, Xi-Ping Jing. Opt. Mater. **75**, 442 (2018).
[20] Ling Li, Shihong Zhou, Siyuan Zhang. Solid State Sci. **10**, 1173 (2008).
[21] A. Szczeszak, T. Grzyb, St. Lis, R.J. Wiglusz. Dalton Transact. **41**, 5824 (2012).
[22] A. Haberer, R. Kaindl, H. Huppertz, Z. Naturforsch. B **65**, 1206 (2010).
[23] R. Velchuri, B.V. Kumar, V.R. Devi, G. Prasad, D.J. Prakash, M. Vital. Mater. Res. Bull. **46**, *8*, 1219 (2011).
[24] Jin Teng-Teng, Zhang Zhi-Jun, Zhang Hui, Zhao Jing-Tai. J. Inorg. Mater. **28**, *10*, 1153 (2013).
[25] S.Z. Shmurak, V.V. Kedrov, A.P. Kiselev, T.N. Fursova, I.I. Zver'kova, E.Yu. Postnova. FTT **63**, *7*, 933 (2021) (in Russian).
[26] S.Z. Shmurak, V.V. Kedrov, A.P. Kiselev, T.N. Fursova, I.I. Zver'kova, E.Yu. Postnova. FTT **63**, *10*, 1615 (2021) (in Russian).
[27] S.Z. Shmurak, V.V. Kedrov, A.P. Kiselev, T.N. Fursova, I.I. Zver'kova. FTT **64**, *4*, 474 (2022) (in Russian).
[28] A.P. Kiselev, S.Z. Shmurak, B.S. Red'kin, V.V. Sinitsyn, I.M. Shmyt'ko, E.A. Kudrenko, E.G. Ponyatovsky. FTT **48**, *8*, 1458 (2006) (in Russian).
[29] S.Z. Shmurak, A.P. Kiselev, N.V. Klassen, V.V. Sinitsyn, I.M. Shmyt'ko, B.S. Red'kin, S.S. Khasanov. IEEE Trans. Nucl. Sci. **55**, *1–3*, 1128 (2008).
[30] S.Z. Shmurak, A.P. Kiselev, D.M. Kurmasheva, B.S. Red'kin, V.V. Sinitsyn. ZhETF **137**, *5*, 867 (2010) (in Russian).
[31] M.A. Elyashevich. Spektroskopiya redkikh zemel. GITTL, M. (1953). 456 p. (in Russian).

[32] M.I. Gaiduk, V.F. Zolin, L.S. Gaigerova. Spektry lyuminestsentsii evropiya. Nauka, M. (1974). 195 p. (in Russian).
[33] D. Hrrniak, E. Zych, L. Kepinski, W. Strek. J. Phys. Chem. Solids **64**, *1*, 11 (2003).
[34] A.G. Ryabukhin. Izv. Chelyabinskogo nauch. tsentra *4*, 33 (2000) (in Russian).
[35] C.E. Weir, E.R. Lippincott. J. RES. Natl. Bur. **65A**, *3*, 173 (1961).
[36] W.C. Steele, J.C. Decius. J. Chem. Phys. **25**, *6*, 1184 (1956).
[37] J.P. Laperches, P. Tarte. Spectrochim. Acta **22**, 1201 (1966).
[38] J.H. Denning, S.D. Ross. Spectrochim. Acta **284**, 1775 (1982).